

DESIGN OF ULTRAFAST IMAGING SYSTEM FOR THYROID NODULE DETECTION

Aarthipoornima Elangovan¹, Jeyaseelan.T²

¹ PG Student, Department of Electronics and Communication Engineering

Kings College of Engineering, Punalkulam, Tamilnadu, Affiliated to Anna University, Chennai, India

² Assistant Professor, Department of Electronics and Communication Engineering

Kings College of Engineering, Punalkulam, Tamilnadu, Affiliated to Anna University, Chennai, India

Abstract - A complete solution to estimate the volume of the thyroid gland directly from ultrasound (US) images is proposed in this paper. Physicians usually diagnose the pathology of the thyroid gland by its volume. However, even if the thyroid glands are found and the shapes are hand-marked from ultrasound images, most physicians still depend on computed tomography (CT) images, which are expensive to obtain, for precise measurements of the volume of the thyroid gland. This approach relies heavily on the experience of the physicians and is very time consuming. Patients are exposed to high radiation when obtaining CT images. In contrast, Ultrasound imaging does not require ionizing radiation and is relatively inexpensive. Ultrasound imaging is thus one of the most commonly used auxiliary tools in clinical diagnosis. The radial basis function neural network is used to classify blocks of the thyroid gland. The integral region is acquired by applying a specific-region-growing method to potential points of interest. The parameters for evaluating the thyroid volume are estimated using a particle swarm optimization algorithm. Simulation results of the thyroid show that the region segmentation can be automatically achieved and the volume of thyroid nodule can be precisely measured.

Key Words: Ultrasound imaging, Thyroid, Thyroid nodule, RBF neural network, PSO algorithm.

1. INTRODUCTION

This paper deals with the concept of medical imaging. Ultra Sonic images are a widely used tool for clinical diagnosis, although it is time consuming for physicians to manually segment the thyroid gland region. The alternative to estimate the volume of a thyroid gland using Computed tomography (CT) imaging is expensive and involves hazardous radiation. Thus, a convenient system for thyroid segmentation and volume estimation in Ultrasound (US) images is of interest. The proposed method includes image enhancement processing to remove speckle noise, which greatly affects the segmentation results of the thyroid gland region obtained from US images.

1.1 Thyroid gland

The thyroid gland is a butterfly shaped organ belonging to the endocrine system and is composed of two cone-like lobes. It controls the secretion of the thyroid hormone, which regulates the temperature of the human body, and greatly affects childhood intelligence, growth, and adult metabolism. Thyroid gland produces hormones that are helpful for the body to control metabolism. Too much or too little thyroid hormone secretion (due to a thyroid that is too large or too small, respectively) causes pathological changes and results in thyroid abnormalities. Therefore, physicians often diagnose abnormal symptoms of the thyroid gland by its volume. The thyroid gland is shown in the figure 1.

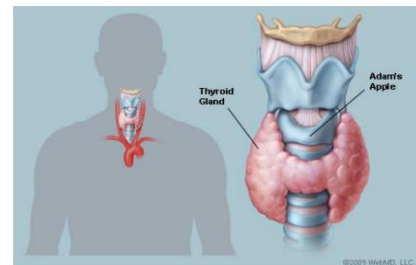


Fig -1: Thyroid Gland

Abnormalities of thyroid function are usually related to production of thyroid hormone. There are four main types of thyroid diseases - hyperthyroidism (too much thyroid hormone), hypothyroidism (too little thyroid hormone), benign (noncancerous) thyroid disease and thyroid cancer (malignant). The thyroid cancerous tissues are cystic or fluid filled when compared to the normal thyroid tissues and they differ in the textural characteristics. The thyroid nodules can be diagnosed by ultrasound imaging

Ultrasound (US) imaging is currently the most popular diagnostic tool. It is inexpensive and easy to use; it can follow anatomical deformations in real time during biopsy and treatment; and it is non-invasive and does not require ionizing radiation.

1.2 Thyroid nodule

The term thyroid nodule refers to an abnormal growth of thyroid cells that forms a lump within the thyroid gland. A thyroid nodule is shown in the figure 2. These are abnormal lumps growing within the thyroid gland which may represent various different conditions including cancer. A thyroid nodule can be non-cancerous (benign) or cancerous (malignant). The most of the thyroid nodules are benign and not cancerous. Digital image processing techniques offer the opportunity for texture description. The thyroid nodule can be characterized by texture description and quantifying properties such as smoothness, coarseness and regularity.



Fig -2: Thyroid nodule image

2. PROPOSED METHODOLOGY

The proposed system focuses on diagnosis of thyroid nodules based on the segmentation of thyroid region and its volume estimation. A complete solution that uses a radial basis function (RBF) neural network to automatically segment the thyroid gland is conceptualised. The Particle Swarm Optimization (PSO) algorithm is then used to estimate the thyroid volume from US images. In the training phase of the network, the physicians manually outline the rectangular regions of interest (ROI) from the thyroid gland and non-thyroid tissues. Six textural features extracted from the ROIs are used to train the RBF neural network. The trained RBF neural network can then automatically roughly classify the thyroid regions from the US images. A specific-region-growing method is then applied to retrieve the complete thyroid region. Finally, based on the area of the segmented thyroid, the thickness, and the depth of thyroid gland, the volume is estimated using a PSO algorithm.

2.1 Advantages of Proposed Methodology

This system incorporates an original methodology that involves a novel algorithm for automatic definition of the boundaries of the thyroid gland. It provides a novel approach for the extraction of noise free image features effectively representing textural properties of the thyroid tissue. Through this extensive experimental evaluation on the real thyroid ultrasound data, the accuracy in thyroid nodule detection has been increased.

- It can automatically segment the thyroid gland region from US images.

- It can accurately estimate the volume of the thyroid from US images

3. SYSTEM IMPLEMENTATION

The diagnosis of thyroid abnormalities involving thyroid region segmentation and volume estimation is carried out using image processing techniques which involves the following steps as shown in figure 3.

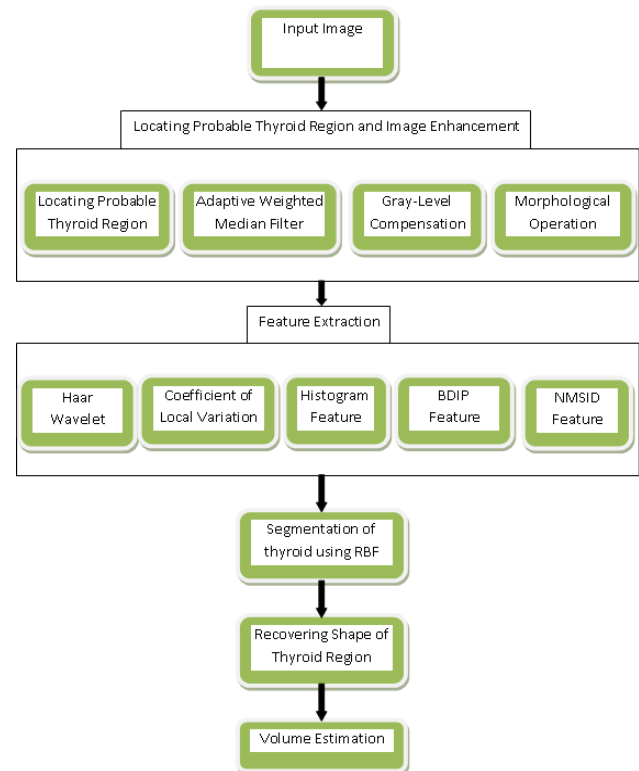


Fig -3: Block diagram of proposed system

3.1 Locating Probable Thyroid Region & Image Enhancement

Locating the probable thyroid region is the first step in detecting the thyroid abnormalities. In thyroid US images, low visual quality greatly affects the segmentation and the volume estimation results. A pre-processing step is thus required to enhance and locate the probable thyroid region. The pre-processing steps are as follows:

- Locating the probable thyroid region
- Applying an AWMF to reduce speckles
- Applying 2 morphological operations to enhance filtering result
- Compensating for different US images according to the intensity template of the thyroid region.

3.2 Feature Extraction

Six discriminative textural features were then extracted from the selected ROIs:

Haar Wavelet Features: The Haar wavelet features are significant features for segmentation in US images.

Mean of LL band:

$$\mu_{x/y} = 1/M^2 \sum_{x/y} eB I(x,y)$$

Variance of LL band:

$$\delta_{x/y}^2 = 1/M^2 \sum_{x/y} eB I(x,y)$$

Where $I(x,y)$ denotes the intensity of a pixel (x,y) in ROI block which passed through the Haar transformation, and B denotes a block size of MXM .

Coefficient of Local Variation Feature : The coefficient of variation (CV) is a normalized measure of dispersion of a probability distribution. Because the texture of thyroid glands differs from those of other regions in the US image, CV is a useful index to represent it.

$$LCV_{x/y} = \frac{\delta_{x/y}}{\mu_{x/y}}$$

Histogram Feature: The histogram feature measures the texture characteristics of an $M \times M$ block. After the pre-processing, the thyroid gland occupies most of the area in the probable thyroid region. Thus, we extract the intensity of the largest area and add a tolerance of ± 10 .

$$HF = \sum_{i=H-10}^{H+10} \text{histo}(i)$$

Where $\text{histo}(i)$ is histogram of a block size of MXM and i is the gray level value.

BDIP Feature: The BDIPs uses local probabilities in image blocks to measure local brightness variations of an image. BDIP is defined as the difference between the number of pixels in a block and the ratio of the sum of pixel intensities in the block to the maximum in the block.

NMSID Feature: NMSID is defined as the differences between the pixel pairs with horizontal, vertical, diagonal, and asymmetric-diagonal directions.

NMSID=

$$\sum_{k=1}^n \left[\sum_{x=0}^{M-1} \sum_{y=0}^{M-k-1} \frac{|I^{x/y} - I^{(x/y+k)}|}{M(M-k)} + \sum_{x=0}^{M-k-1} \sum_{y=0}^{M-1} \frac{|I^{x/y} - I^{(x+k/y)}|}{M(M-k)} + \sum_{x=0}^{M-k-1} \sum_{y=0}^{M-k-1} \frac{|I^{x/y} - I^{(x+k/y+k)}|}{M-k^2} + \sum_{x=0}^{M-k-1} \sum_{y=0}^{M-k-1} \frac{|I^{x/y} - I^{(x-y+k)}|}{M-k^2} \right]$$

/4

where $I(x,y)$ denotes the intensity of a pixel (x,y) in a block with a size of $M \times M$ and n denotes the maximum horizontal or vertical distance.

3.3 Segmentation of thyroid region by RBF

Image segmentation is the process of partitioning an image into multiple segment or set of pixels used to locate object and boundaries.

3.4 RBF(Radial Basis Function) neural network

RBF neural networks have attracted a lot of attention due to their good reliability in the field of image classification. A RBF neural network as shown in figure 4 includes one hidden layer, which has high dimensionality. The trained RBF neural network classifies the block into the thyroid gland and the non-thyroid gland. For each thyroid block, the number of thyroid blocks was calculated in its 8-nearest neighbors. If the number is smaller than four, the block is reassigned to non-thyroid glands. Finally, the largest connected component is extracted from the classified US image. The region of the largest connected component is considered as part of the thyroid gland region.

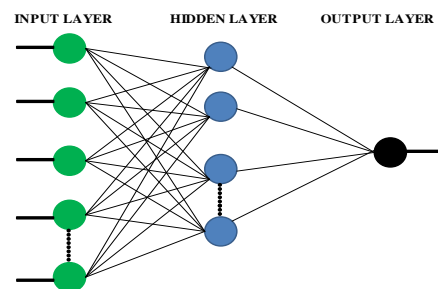


Fig -4: Radial Basis Function neural network

3.5 Recovering Shape of Thyroid Region

Using the aforementioned procedures, a pure region of the thyroid gland can be extracted (i.e., no pixels belong to the non-thyroid gland region). However, the shape of the segmented thyroid region is serrated, and thus, a refinement procedure is required to recover the complete thyroid gland region. Consequently, three specific reconstruction stages are applied to recover the complete shape of the thyroid gland. The first reconstruction stage is filtering out the blocking shape of the segmented thyroid region. The second reconstruction stage is based on the convex-hull concept.

3.6 Volume Estimation

Since computed tomography (CT) imaging is expensive and involves hazardous radiation, US imaging is the most

commonly used auxiliary tool currently utilized in clinical diagnosis. Hence, this study proposes a complete solution to estimate the volume of the thyroid gland directly from US images.

3.7 PSO (Particle Swarm Optimization) algorithm

PSO is a population-based stochastic optimization technique used to obtain a set of potential solutions that evolves to approach a convenient solution (or set of solutions) for a problem. The PSO algorithm has been reported to have strengths of fast convergence and robust stability over other evolutionary optimization mechanisms, such as genetic algorithms or ant colony algorithms. Therefore, the PSO algorithm is applied to estimate the parameters of the thyroid volume equation. With this optimization scheme, the scale and bias parameters for volume estimation can be directly estimated from the US images.

4. SIMULATION RESULTS

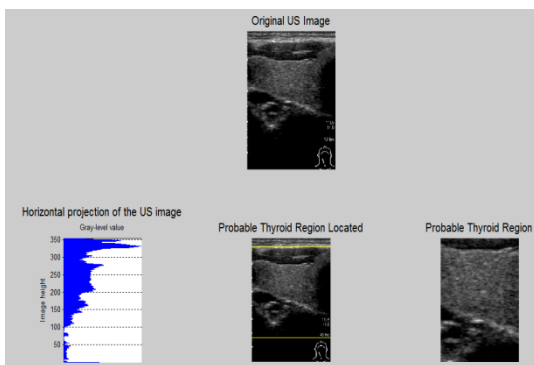


Fig 5: Detection of thyroid region

OBSERVATION : Histogram equalization provides the probable thyroid region as shown in Fig.5.



Fig 6: Gray level compensation

OBSERVATION : Gray level compensation is carried out on the image to adjust the intensity of the image as in the above Fig 6.

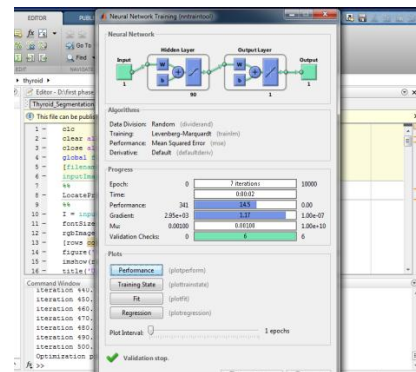


Fig 7: Neural network processing

OBSERVATION : Then the image is processed in the RBF neural network tool as in the above figure for segmentation and volume estimation. The trained RBF neural network classifies the block into the thyroid gland and the non-thyroid gland.

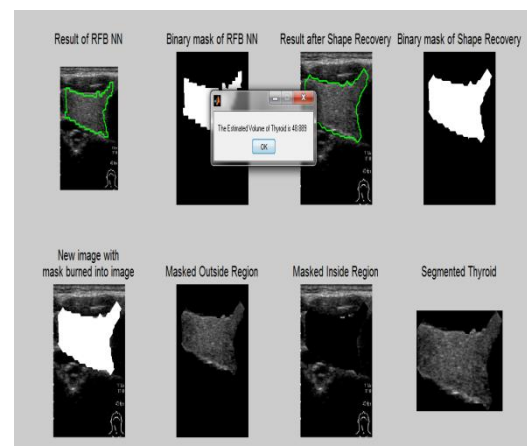


Fig- 8: Volume estimation

OBSERVATION : The thyroid image from the RBF neural network is obtained and it is masked using binary masking and the shape of the thyroid region is recovered. The parameters such as area, thickness and the depth of thyroid gland are computed from the segmented thyroid region and the volume is estimated

5. CONCLUSION

In this paper, an effective diagnosis of thyroid abnormalities based on image processing techniques is discussed. Segmentation of the thyroid region and volume estimation are explained. The diagnosis is carried out by considering features such as area of segmented region, depth, thickness, volume etc. US images are a widely used tool for clinical diagnosis, although it is time consuming for physicians to manually segment the thyroid gland region. The alternative to estimate the volume of a thyroid gland using CT imaging is expensive and involves hazardous radiation. Thus, a

convenient system for thyroid segmentation and volume estimation in US images is of interest.

The proposed method includes image enhancement processing to remove speckle noise, which greatly affects the segmentation results of the thyroid gland region obtained from US images. The probable thyroid gland region is located in the US image, and then, an RBF neural network is used to classify the region into thyroid and non-thyroid gland areas. Finally, a region growing method is applied to recover an accurate shape of the thyroid gland region. The experiment results show that the proposed method can be used to segment the thyroid gland region and to estimate thyroid volume directly from US images. The proposed method offers two significant improvements: 1) it can automatically segment the thyroid gland region from US images and 2) it can accurately estimate the volume of the thyroid from US images.

REFERENCES

- [1] Abraham A., Guo H. and Liu H. (2006), 'Swarm intelligence: Foundations, perspectives and applications', in *Swarm Intelligent Systems, Studies in Computational Intelligence*, Vol. 26, pp. 3–25.
- [2] Baillard C., Barillot C. and Bouthemy P. (2000) Nov, 'Robust adaptive segmentation of 3d medical images with level sets', Institut National de Recherche en Informatique et en Automatique (INRIA), Le Chesnay Cedex, France, Tech. Rep. 4071.
- [3] Brunn J., Block U., Ruf G., Bos I., Kunze W. P. and Scriba P. C. (1981) Oct, 'Volumetric analysis of thyroid lobes by real-time ultrasound', *Dtsch Med Wochenschr*, Vol. 106, pp. 1338–1340.
- [4] Chen Y., Yin R., Flynn P., and Broschat S. (2003) Feb, 'Aggressive region growing for speckle reduction in ultrasound images', *Pattern Recognit. Lett.*, Vol. 24, pp. 677–691.
- [5] Chen D. R., Chang R. F., Wu W. J., Moon W. K., and Wu W. L. (2003) Jul, '3-D breast ultrasound segmentation using active contour model', *Ultrasound Med. Biol.*, Vol. 29, no. 7, pp. 1017–1026.
- [6] Chen E. L., Chung P. C., Chen C. L., Tsai H. M., and Chang C. I. (1998), 'An automatic diagnostic system for CT liver image classification', *IEEE Trans. Biomed. Eng.*, Vol. 45, no. 6, pp. 783–794.
- [7] Chiu B., Freeman G. H., Salama M. M. A., and Fenster A. (2003) Sep, 'Prostate segmentation algorithm using dyadic wavelet transform and discrete dynamic contour', *Phys. Med. Biol.*, Vol. 49, no. 21, pp. 4943–4960.
- [8] Chum Y. D. and Seo S. Y. (2004) Nov, 'Image retrieval using BDIP and BVLC moments', *IEEE Trans. Circuits Syst. Video Technol.*, Vol. 13, no. 9, pp. 951–957.
- [9] Clerc M., (2006) Standard PSO version. http://www.particleswarm.info/Standard_PSO_2006.c
- [10] Eberhart R. C. and Kennedy J. (1995) Oct, 'A new optimizer using particle swarm theory', in *Proc. 6th IEEE Int. Symp. MicroMach. Human Science*, pp. 39–43.